J. Phys. A: Math. Theor. **44** (2011) 075101 (15pp) doi:10.1088/1751-8113/44/7/075101

Competitive trapping in complex state spaces

Andreas Fischer[1,2,3], **Karl Heinz Hoffmann**[1] **and J Christian Schön**[4]

[1] Institut für Physik, Technische Universität Chemnitz, 09107 Chemnitz, Germany
[2] Küberneetika Instituut, Tallinna Tehnikaülikool, 12618 Tallinn, Estonia
[3] Department of Physics, Mu'tah University, Al Karak, Jordan
[4] Max-Planck-Institut für Festkörperforschung, Heisenbergstraße 1, 70569 Stuttgart, Germany

E-mail: andreas.fischer@physik.tu-chemnitz.de

Received 2 September 2010, in final form 29 November 2010
Published 21 January 2011
Online at stacks.iop.org/JPhysA/44/075101

Abstract
In complex state space dynamics at finite time scales, the trapping in certain regions of state space is of great importance, e.g. in the field of protein folding or in the application of stochastic global optimization algorithms. Here, we analyze the influence of the density of states on the features of the trapping process. In particular, we compare the trapping power of a valley with a power-law density of states to one with an exponentially growing density of states. The outcome of this competition crucially depends on the annealing speed and shows that the clear difference between these two paradigmatic densities of states observed at very slow (near-equilibrium) annealing is lost for fast non-equilibrium processes, and that the outcome of the relaxation can strongly depend on the time scale of the process and subtle features of the density of states.

PACS numbers: 82.20.Db, 31.70.Hq

1. Introduction

Understanding the dynamics on energy landscapes provides the basis for the successful modeling of a large variety of experimental findings [1–4]. A particularly useful tool is the so-called master equation dynamics. It can be used to model the thermally activated relaxation process of the system toward equilibrium as a Markovian probability flow if the energy landscape can be represented as a hierarchical tree structure. Quite generally, lowering the temperature during a relaxation process drives the system deeper into the valley structure of the energy landscape. But in many systems, it is found that some of the local minima seem to attract more probability than expected compared to other regions of the state space, and this phenomenon has been called *preferential trapping* [5].

Understanding preferential trapping from an application-related point of view is a yet unsolved problem in many fields of complex system dynamics. Especially the folding of

proteins into their functionally necessary structures is still an open question [6], as much as the sweeping success of stochastic optimization methods such as simulated annealing [7–9]. As further examples, preferential trapping in stable energy minima is also essential in the dynamics of chemical reactions, which is reflected for instance in the success of retrosynthesis [10], the formation of amorphous [11] and crystalline solids [12], and the creation of clusters [13]. In all of these cases the dynamical evolution of the system is controlled by the energy of the states as well as by the topology of the (usually) rough landscape where many local minima are separated by a large number of barriers of different heights.

The standard analysis of e.g. the simulated annealing algorithm is based on establishing a Boltzmann distribution over the state space of a system [9, 14]. This results in an increased population of energetically low-lying states when decreasing the temperature T during the relaxation. Thus, for $T = 0$ one would expect the system to be in the global minimum of the whole state space. However, the time scales available for simulating this process in actual algorithmic implementations appear to be much too short compared to the times expected according to global equilibrium considerations [9, 14]. Nonetheless, practical applications of simulated annealing show that the chance of finding the ground state in a relatively short time is quite high. Similarly, in protein folding, the functionally important structures correspond to low-lying local minima of the energy function of the system, and despite the huge size of the state space, folding occurs in very short times, the so-called Levinthal's paradox [15]. To account for this, concepts like funneling on energy landscapes [16] have been developed in the past.

For such processes that occur on very short time scales compared to those required according to equilibrium considerations, the fast progress toward energetically low lying states needs to be supported by the local state space structure at branching points, i.e. saddles/transition regions of the landscape, of the probability flow. That is the basis of the so-called *deep valleys have large rims* hypothesis [9]. It is based on the argument that the probability for entering one of two valleys at a saddle point is proportional to the respective number of states right below that saddle region where the valleys separate, i.e. the rim size of the valley. As a consequence, if the hypothesis holds, the system would be drawn toward its low-lying local minima even for very fast annealing. However, simulated annealing shows amazing success even in the cases where the hypothesis cannot be applied.

Obviously, in the above processes some further funneling mechanisms must be present. In an earlier work, these preferential trapping phenomena have been analyzed with regard to the competitive behavior between *energetic* and *entropic* (e.g. density of states) features [5]. Later, the analysis was extended, demonstrating that the movement on energy landscapes is also substantially governed by a third aspect, the *kinetic* features of the landscape [17]. These are closely connected to the local connectivity in the state space, since kinetic features describe how easily a system can move between regions of the state space. Within the picture of a mountainous landscape, one can visualize kinetic barriers as the width of the pass between two valleys.

As a consequence, energetic, entropic and kinetic features can be put on a general equivalent footing when viewed in terms of their influence on the probability flow on an energy landscape [18–23]. In all of the above analyses the focus was on systems with exponentially increasing local densities of states, since such valleys had been observed in a number of complex systems analyzed in theory [24, 25] and application [11, 26, 27]. It could be shown that at a critical temperature T_{trap} a dynamic phase transition [5, 11] occurs, where the most likely location of the random walker switches between the bottom and the top of the valley, irrespective of the valley's depth. However, many complex systems exhibiting subexponential power-law-like increasing local densities of states have also been observed

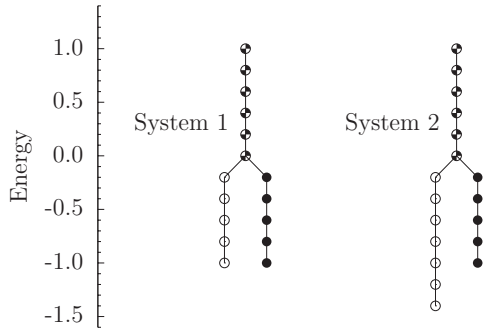

Figure 1. For the analysis of preferential trapping, we use a model system consisting of two valleys of a complex energy landscape embedded in a super-valley. The energetic, entropic and kinetic features of the landscape are herein represented by the depth of the valleys, the degeneracies of the nodes and the transition probabilities between connected nodes.

[28–30] that can show 'fast annealing' behavior. Of course, pure exponential and power-law increases are paradigmatic limit cases, while in real systems valleys with increases closer to one or the other type are usually observed, with quite some variability even within a single system.

Thus, the question arises, whether an exponentially increasing local density of states is actually a necessary condition for observing preferential trapping. In order to address this issue, we have analyzed the probability flow in competing valleys that exhibit power-law and exponential growth in the local densities of states. Based on a hierarchical tree model we analyze the dynamic behavior of a simple prototypical system, in particular the crossing of barriers at individual saddle points of the landscape. The influence of various parameters like energetic depth, density of states and connectivity of the valleys are studied for both isolated and interacting valleys. We find that preferential trapping also occurs in systems with a power-law increase of the local density of states for fast annealing. Furthermore, we observe competing effects of the energetic, entropic and kinetic features, which can lead to inversions of the final occupation probabilities of the valleys as a function of the annealing speed.

2. A simplified state space model

In order to demonstrate the competing influence of energetic, entropic and kinetic features on the dynamics of random walkers in state space, we employ a simplified state space model governed by master equation dynamics. The model describes two valleys which are connected to a higher-lying region. This region will be dubbed *super-valley* as the model is considered to represent a subregion in a large tree-like energy landscape.

From a technical point of view, it is advantageous to subdivide the valleys into slices along the energy axis. Thus, the model is composed of a number of nodes in a chain-like structure as shown in figure 1. Two major versions of the model are studied: one consisting of valleys of equal depth (S1) and one consisting of two valleys with different depths (S2) having a local minimum in valley 1 and a global minimum in valley 2. Without loss of generality, the reference minimum in valley 1 is placed at $E_{\min}^{(1)} = -1$ and the saddle where the two valleys split at $E_{\text{saddle}} = 0$. For system S1, the nodes in both valleys can be found at energy levels $(-1.0, -0.8, -0.6, -0.4, -0.2)$, and in the super-valley at (0.0, 0.2, 0.4, 0.6, 0.8, 1.0). For system S2 there are two additional nodes in valley 2 at $(-1.2, -1.4)$.

The nodes of the models exhibit a certain degeneracy, since they represent coarse-grained slices of the state space containing many states. The accumulation of these micro-states into one macro-state is possible as the slices are assumed not to contain any energetic barriers. The resulting degeneracies capture the important entropic features of the landscape. In this paper we discuss two paradigmatic densities of states, one growing exponentially and one with a power-law, respectively; as noted above, a wide range of observed densities of states are covered by these functional forms. Some of the equilibrium and non-equilibrium features of the dynamics associated with one or the other of these densities of states have already been discussed in earlier work [5, 17, 31] but not the consequences of combining such valleys.

On the one hand, the degeneracy $g^{(\alpha)}(E)$ in valley α is chosen here as exponentially increasing

$$g^{(\alpha)}_{\mathrm{exp}}(E) = g^{(\alpha)}_{\mathrm{min}} \exp\left[\frac{E - E^{(\alpha)}_{\mathrm{min}}}{T^{(\alpha)}_{\mathrm{tr}}}\right], \tag{1}$$

where $g^{(\alpha)}_{\mathrm{min}}$ and $E^{(\alpha)}_{\mathrm{min}}$ represent the degeneracy and the energy of the minimum node in valley α, respectively, and the inverse growth factor $T^{(\alpha)}_{\mathrm{tr}}$ is the so-called trapping temperature [5, 26]. On the other hand, $g^{(\alpha)}(E)$ is chosen as a power-law:

$$g^{(\alpha)}_{\mathrm{pow}}(E) = g^{(\alpha)}_{\mathrm{min}}\left(\frac{E - E^{\mathrm{global}}_{\mathrm{min}} + \Delta E}{E^{(\alpha)}_{\mathrm{min}} - E^{\mathrm{global}}_{\mathrm{min}} + \Delta E}\right)^{\gamma}, \tag{2}$$

where γ is the power-law's exponent, ΔE is the width of an energy slice and $E^{\mathrm{global}}_{\mathrm{min}}$ is the energy of the whole system's minimum node which needs to be included for technical reasons to ensure that the expression inside the brackets is always positive, and thus proper scaling in a power-law regime is achieved. Nonetheless, there are other choices possible [32]. In principle, the equilibrium thermal properties of valleys with a power-law density of states and those with an exponentially increasing density of states are rather different. Valleys with an exponentially increasing density of states show a critical temperature—the trapping temperature—at which the equilibrium probability distribution inside the valley abruptly changes from exponentially decreasing to exponentially increasing, with increasing energy. This implies that for temperatures above the critical temperature most of the probability will be outside the valley; in other words, the valley is not seen by the system. For details see [5]. In contrast, valleys with a power-law density of states show a gradual decrease of probability starting at the bottom and advancing to the rim of the valley at increasing temperature. This means that the probability is not squeezed out of or sucked into the valley at one critical temperature but the change in the equilibrium probability distribution is continuous as a function of temperature.

The last ingredient for the system description is the so-called mobility, i.e. the number of micro-connections between the states. Those states connected by many different pathways will have a larger transition probability between them than those with few micro-connections. In the coarse-grained model this feature is modeled via the kinetic factors $f^{(\mathrm{kin})}_{ij}$ for the transition between nodes [33, 34]. These kinetic factors determine the time scale on which probability moves between the nodes. In the following analyses, only the ratios of these different kinetic factors are physically important.

Combining all the above-mentioned parts, we derive a master equation describing the dynamics of the model in a Metropolis–(Markovian)-like manner [35]:

$$P^{(t+1)}_i = \sum_{j=1}^{N} \Gamma_{ij}(T^{(t)})\, P^{(t)}_j, \tag{3}$$

where N is the total number of nodes and $P_i^{(t)}$ is the probability to be in node i at time step t. The nondiagonal elements of the transition matrix $\Gamma_{ij}(T^{(t)})$ are nonzero only for those pairs of nodes which are directly connected by an edge as shown in figure 1. In this case they are given by the Metropolis rates along the edge

$$\Gamma_{ij}(T^{(t)}) = \begin{cases} f_{ij}^{(\mathrm{kin})} \dfrac{g(E_i)}{g(E_j)} \exp\left(\dfrac{-\Delta E}{k_B T^{(t)}}\right) & i \neq j, E_i > E_j \\ f_{ij}^{(\mathrm{kin})} \dfrac{g(E_i)}{g(E_j)} & i \neq j, E_i \leqslant E_j \\ 1 - \displaystyle\sum_{k \neq j} \Gamma_{kj} & i = j, \end{cases} \tag{4}$$

where ΔE is the corresponding energy difference.

Note that only the ratio Γ_{ij}/Γ_{ji} is determined by the energy differences and the densities of states of the system via the detailed balance requirement. However, the absolute values of the rates, which determine the time scale for the equilibration between the two nodes, are not predetermined by the degeneracies but are controlled by the kinetic factors $f_{ij}^{(\mathrm{kin})} = f_{ji}^{(\mathrm{kin})}$.

For the annealing, we use a schedule which decreases the temperature linearly in N steps from an initial T_i to a final T_f. The number of Metropolis moves at a given temperature is M. Finally, quenching a distribution is equivalent to evolving it with the master equation for $T = 0$ until no probability remains outside the two minima. The outcome of such a quench is denoted as the 'quenched probability'. We also used a schedule which decreases the temperature exponentially; however, the general qualitative features presented below did not change.

3. Results

3.1. Trapping experiments

As a preliminary step, the trapping behavior of two-subvalley systems with an exponential and a power-law density of states in both subvalleys, respectively, is investigated. The first case (case A) consists of two valleys of equal depth (tree structure S1), with exponentially increasing densities of states and identical kinetic factors, the difference being the trapping temperatures $T_\mathrm{tr}^{(1)} = 0.4/\log(2) \approx 0.58$ for valley 1 and $T_\mathrm{tr}^{(2)} = 0.2/\log(2) \approx 0.29$ for valley 2. The degeneracy in the super-valley (where the two valleys are merged) also grows exponentially with $T_\mathrm{tr}^{(\mathrm{SV})} = 0.2/\log(2) \approx 0.29$ as shown in figure 2 (top left). The number of moves M at each temperature varies over the range $M \in [1 \cdots 2^{20}]$ with a fixed number of temperature steps $N = 10$ from $T_\mathrm{i} = 0.6$ to $T_\mathrm{f} = 0.05$. The initial probability distribution is concentrated in the top node of the super-valley.

In figure 2 (middle left) the development of the probabilities as a function of M is shown. The quenched probabilities of the initial distribution differ due to the different likelihood for entering one of the two valleys which is proportional to the respective rim size or degeneracy just below the separation point. On the other hand the final equilibrium distribution represents the degeneracies inside the respective valleys since the final temperature is small and thus the remaining probability in high-lying states of the super-valley is negligibly small. Note that the equilibrium distribution at temperature $T = 0$ gives equal probabilities for both valleys since their bottom nodes are equal in degeneracy and energy. Figure 2 (middle left) clearly shows the expected transition from the quenching-like behavior for fast schedules to the equilibrium-like behavior for slow schedules.

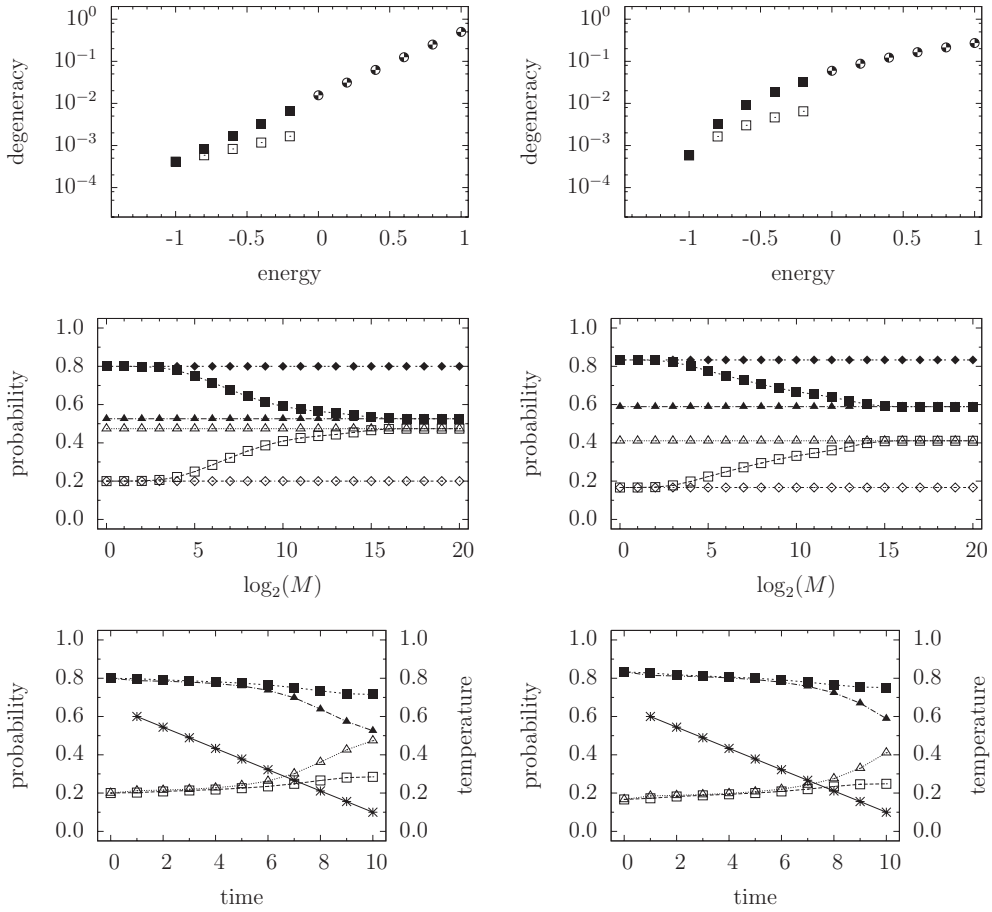

Figure 2. The degeneracy versus energy (top), the quenched probability distribution as a function of the number M of Metropolis moves between temperature updates (middle) and the time development of the probabilities (bottom) for cases A (left) and B (right). In the middle panels, the probability distribution for finding a random walker in valley 1 (open symbols) or valley 2 (filled symbols) is shown. The boxes represent the probabilities obtained from iterating the master equation according to a linear temperature schedule and afterward quenching the system down. For comparison, diamonds depict the probability distribution after quenching the initial state, and triangles represent the outcome of quenching the equilibrium probability distribution at the final temperature (of course, these distributions do not depend on M). In the bottom panels, the time development of the probabilities is shown for a linear temperature schedule (symbol: stars; ordinate on the right). The open/filled boxes represent the quenched probability inside valleys 1 and 2, respectively, of the annealing process. For comparison, the open/filled triangles depict the quenched equilibrium probability distribution at current temperature for valleys 1 and 2, respectively. Time is measured in units of temperature updates, with $M = 2^7$ Metropolis steps at each temperature.

Figure 2 (bottom left) shows the probability flow into the valleys as a function of time (where time is counted in temperature steps) for $M = 2^7$ Metropolis moves between temperature steps. At high temperatures the probability distribution stays equilibrated, but once the first valley's trapping temperature is reached ($t \approx 5$) differences between annealing data and equilibrium data appear. When the temperature drops below the second valley's trapping temperature (at $t \approx 7$), equilibrium is completely lost. Below this point the system increasingly behaves like being quenched. These results agree with earlier work [17].

Next, we consider a system (tree structure S1) with power-law degeneracies in all parts of the valley (case B). The exponents of the power-laws are $\gamma^{(1)} = 1.5$ for valley 1, $\gamma^{(2)} = 2.5$ for valley 2 and $\gamma^{(SV)} = 2.5$ for the super-valley, respectively (cf figure 2 (top right)). Compared to figure 2 (top left), there is a smaller increase of the degeneracy at high energy levels as well as a stronger increase at low energy levels.

Figure 2 (middle right) shows the probabilities as a function of M for the same linear temperature schedule. The behavior is very similar to the case of exponential growth. The probabilities obtained by quenching the initial distribution differ due to the different likelihood for entering one of the two valleys which is proportional to the respective rim size or degeneracy just below the separation point. On the other hand the final equilibrium distribution represents the degeneracies inside the respective valleys since the final temperature is small and thus the remaining probability to be in high-lying states is negligibly small. Again, we find a smooth change from a quenching-like behavior for fast schedules (M small) to an equilibrium-like behavior for slow schedules (M large). This is the expected behavior as the slower the annealing proceeds, the better a local equilibrium around the saddle point can be established.

Similarly, figure 2 (bottom right) shows the probability flow as a function of time for $M = 2^7$ single Metropolis moves between temperature steps. While at high temperatures the distribution is equilibrated, deviations appear at intermediary temperatures ($t \approx 5$, $T = 0.38$) although no trapping transition of the equilibrium distribution as such exists for power-law growth of the densities of states in a single valley. When the temperature drops even lower ($t \approx 7$, $T = 0.27$), equilibrium is completely lost, and the system behaves essentially as if it had been quenched.

In summary, we find that a pure power-law growth of the degeneracies leads to a behavior very similar to the one for a pure exponential setup. One further point worth mentioning is that the system with a power-law growth appears to get closer to its equilibrium distribution for smaller values of M than with an exponential growth. This behavior can probably be explained by the fact that in the exponential case there exists an underlying critical temperature for each valley at which the proper annealing speed should be matched for optimal convergence toward the equilibrium distribution.

These observations are rather general and do not critically depend on the number of states or the particular energy steps of the model, as was seen when the calculations were repeated, both for higher energy resolution and for exponentially decreasing temperature during the annealing. Of course, the results do vary with the parameters of the model, but even if the density of states changes by a factor of 10^5, an appropriately rescaled temperature ramp shows similar results.

3.2. A simple chain of states

To understand the unexpected similarities between valleys with exponential and power-law densities of states, we analyze the probability distribution in a single valley (i.e. along a simple chain of states) in thermal equilibrium as well as in non-equilibrium during a quench to a fixed temperature.

For systems with an exponentially increasing density of states, the equilibrium probability density (per energy interval) exponentially decreases from the top to the bottom of the valley at a temperature $T > T_{\mathrm{tr}}$, while at $T < T_{\mathrm{tr}}$ the probability density increases, i.e. at $T > T_{\mathrm{tr}}$ the valley repels a walker while at $T < T_{\mathrm{tr}}$ the valley traps the walker, respectively. For a chain of 21 nodes without any branches (ranging in energy from $E_{\mathrm{min}} = -1.0$ to $E_{\mathrm{max}} = 1.0$), the equilibrium probability density versus the energy of the states is shown in figure 3 (left) for a range of temperatures.

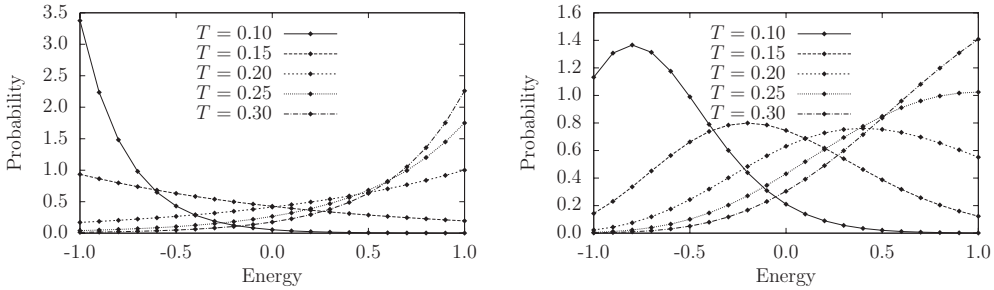

Figure 3. The probability distribution versus the energy of the states for a simple system in equilibrium at various temperatures. Left: exponential setup, right: power-law setup.

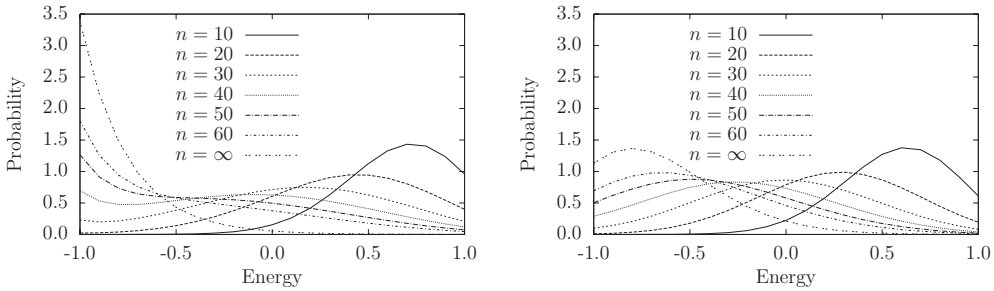

Figure 4. The probability distribution versus the energy of the states is shown for the simple test system after a quench of n steps to $T = 0.10$ energy units for several relaxation times. Left: exponential setup, right: power-law setup.

In contrast, for systems with a power-law density of states, the probability density shows a peak that is successively shifted to lower energies by decreasing the environment temperature T (see figure 3 (right)).

However, in non-equilibrium situations, these distributions look different. In figure 4, we show the probability distributions for the above systems (prepared to reside in the topmost state at starting time) after a (short) relaxation at a temperature $T = 0.1$, where the number of relaxation steps will be denoted by n. During the relaxation, probability is being transported downward, and for both densities of states, one observes a probability peak that moves toward lower energies. Both distributions look very similar as long as the values of n are not too large; however, for long relaxation times, we recover the differences observed in the equilibrium distributions (of course, the meaning of 'long' is dependent on the other system parameters). But as long as the probability flow within the system is large we observe a strong similarity for both systems.

3.3. Kinetic factors and valley depth

In the following case C (cf figure 5 (left)), we extend the results obtained in [17] for the competition of energetic and kinetic factors.

The underlying tree structure is S2, see figure 1, with trapping temperatures $T_{\mathrm{tr}}^{(1)} \approx 0.259$, $T_{\mathrm{tr}}^{(2)} \approx 0.563$ and $T_{\mathrm{tr}}^{(SV)} \approx 0.597$. The shallower valley 2 starts with a degeneracy at its bottom which is 18 times as large as the one of valley 1, while the kinetic factors are the same in

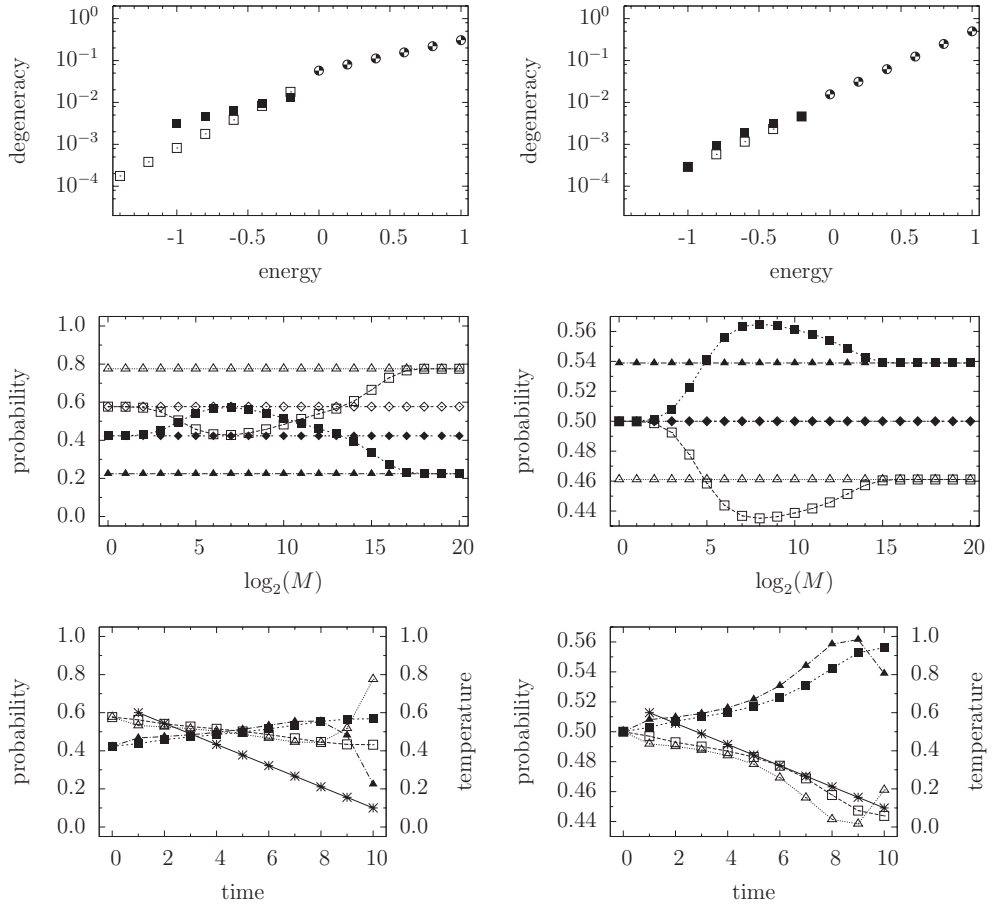

Figure 5. The degeneracy versus energy (top), the quenched probability distribution as a function of the number M of Metropolis moves between temperature updates (middle) and the time development of the probabilities (bottom) for cases C (left) and D (right). For notation, see figure 2.

both valleys. Thus, valley 2 has a slightly smaller rim size than valley 1, but below the rim, valley 2 shows a higher degeneracy on all levels than valley 1. The total number of states in both valleys is the same; the fact that valley 1 is deeper than valley 2 mainly influences the equilibrium distribution at low temperatures.

The temperature decreases linearly from $T_\mathrm{i} = 0.6$ to $T_\mathrm{f} = 0.05$ in ten steps, with $M \in [1 \cdots 2^{20}]$ moves performed at each temperature step. As one can see in figure 5 (middle left), both quenching the initial distribution (corresponding to $M = 0$) and a very fast annealing ($M < 2^4$) lead to a higher quenched probability in valley 1, due to its bigger rim. However, if the annealing process is a bit slower ($M = 2^4 \cdots 2^{10}$), the mobility is still high enough compared to the annealing speed for valley 2 to attract probability as soon as the temperature drops below its trapping temperature. But for $M > 2^{10}$, valley 1 can also draw a considerable amount of probability as the temperature reaches its trapping temperature, and, due to its greater depth, valley 1 can supersede valley 2.

Analyzing the dynamical behavior at an intermediate annealing speed ($M = 2^7$, as depicted in figure 5 (bottom left)), one finds that at high temperatures the quenched probability

is concentrated in valley 1. Once the temperature falls below the trapping temperature of valley 2, the probability is funneled into valley 2. But when the trapping temperature of valley 1 is reached, the situation reverses again as the equilibrium curves (symbol: triangle) show. However, for $M = 2^7$ the mobility is too low and the probability can no longer be transferred from valley 2 to valley 1.

Thus, both for quenching ($M = 0$) and for quasi-equilibrium ($M \approx \infty$) a random walker will end up in the deepest valley (1) with high probability, but for an intermediate range of annealing speeds the walker will end up in a local minimum (valley 2). This result contradicts the usual assumption that the likelihood of finding the global minimum during annealing monotonically increases with the length of the simulation [9] or the duration of the chemical/physical process.

3.4. Competition between exponential and power-law valleys

We next examine case D (tree structure S1) with both valleys (1 and 2) having equal degeneracy at their lowest as well as at their topmost nodes; however, valley 1 has an exponentially increasing density of states while valley 2 exhibits power-law DoS, respectively. The trapping temperatures of valley 1 and the super-valley are $T_{\mathrm{tr}}^{(1)} = T^{(\mathrm{SV})} \approx 0.289$. Since the parameters of valley 2 are chosen to match the above requirements, the degeneracy of valley 2 is higher than the one of valley 1 at all nodes (cf figure 5 (top right)).

Again we linearly decrease the temperature from $T_{\mathrm{i}} = 0.6$ to $T_{\mathrm{f}} = 0.05$ in ten steps with $M \in [1 \cdots 2^{20}]$ moves performed at each temperature step. As one can see in figure 5 (middle right), quenching the initial distribution leads to a completely symmetric probability distribution as in this case only the two valleys' equal rim sizes are relevant. In contrast, for the quenched equilibrium distribution at the final temperature we find more probability in valley 2 (filled symbols) because the final temperature is not zero and thus a finite amount of probability is located at nodes above the minima and thus valley 2 attracts more probability due to its higher degeneracy. For very low or very high annealing speeds, the quenched probability resembles the one for equilibrium or quench, respectively. However, at an intermediate annealing speed (around $M = 2^7$), valley 2 contains more probability than it would attract in equilibrium at the final temperature. The cause of this effect is that, due to the non-vanishing annealing speed, a probability exchange between both valleys mainly takes place at the temperature where most probability resides in the nodes just below the saddle region. However, at these energies, the local densities of states of valleys 1 and 2 favor the power-law valley even more strongly than at the energy levels just above the minima.

The time evolution of the probabilities at an intermediate speed depicted in figure 5 (bottom right) also shows that the system is controlled by two competing effects: any downward flowing probability is distributed evenly due to the valleys' equal rim sizes, while the power-law density of states just below the separation point is much higher than the exponential DoS. Following the curves we find that at higher temperatures the 50–50 effect is quite noticeable as the quenched equilibrium assigns actually more probability to valley 2 than the annealing process does by itself. From this example, we conclude that in many situations a power-law valley can draw more probability than a similar exponentially governed valley, due to its higher total state space volume.

We now turn to an example (case E) which shows a competition of energetic, entropic and kinetic effects for a power-law valley versus an exponential valley. We employ a tree of type S2, where valley 1 exhibits an exponentially increasing degeneracy and has its energetic minimum at $E_{\mathrm{min}}^{(1)} = -1.4$. In contrast, valley 2 shows a power-law increase in degeneracy, starting with a degeneracy at its minimum ($E_{\mathrm{min}}^{(2)} = -1.0$) which is 22 times larger than

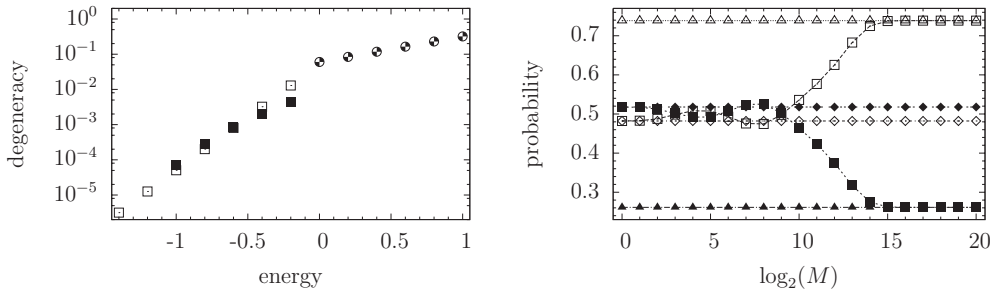

Figure 6. The degeneracy versus energy (left), and the quenched probabilities as a function of M (right) for case E. Notation as in figure 2.

the one of valley 1. The trapping temperature of valley 1 is set to $T_{\rm tr}^{(1)} \approx 0.144$ and the trapping temperature of the super-valley is $T_{\rm tr}^{(\rm SV)} \approx 0.597$, while the parameters of valley 2 are chosen to make the size of the rim of valley 2 34% of the rim size of valley 1. As a consequence, at energies below $E = -0.5$, valley 2 has a higher degeneracy than valley 1, and at energies above $E = -0.5$, the situation is reversed. In addition, the mobility in valley 1 is set equal to 32% of the mobility of valley 2. Note that in figure 6 (left) only the degeneracy is presented; the differences in kinetic factors influence the apparent rim size when a quench is performed.

Again, we linearly decrease the temperature from $T_{\rm i} = 0.6$ to $T_{\rm f} = 0.05$ in ten steps with $M \in [1 \cdots 2^{20}]$ moves performed at each temperature step. As depicted in figure 6 (right), we find a quite complex behavior where the quenched probability shows two inversions as a function of M.

Quenching and very fast annealing ($M < 2^3$) leads to a slightly higher probability (0.52 versus 0.48 for the quench) in valley 2 due to its advantage in mobility, which overcompensates the higher rim size of valley 1 (the mobility in valley 1 is 32% of the one in valley 2, but the rim size of valley 2 is 34% of the one of valley 1). However, if the annealing process is run a bit more slowly ($M = 2^4 \cdots 2^5$), the higher degeneracy of valley 1 just below the separation point becomes important, and thus more probability is attracted by valley 1. But if the annealing proceeds even more slowly ($M = 2^6 \cdots 2^9$), the mobility combines with the greater state space volume of valley 2 compared to valley 1 at energy levels below $E = -0.5$ to successfully accumulate probability in valley 2. Finally, at very low annealing speeds ($M > 2^{10}$) the mobility is still high enough that probability can be transported into valley 1, at the time when the temperature drops below valley 1's trapping temperature. One should note that the actual occurrence of such a complex behavior sensitively depends on the parameters of the model. However, the general qualitative features discussed in this work do not depend on e.g. whether the temperature schedule is exponential or linear. In summary, the interaction between an exponential valley and a power-law valley leads to many new and interesting features which get even more pronounced if additional asymmetries in kinetics and valley depth are present.

However, one might argue that in the examples discussed above the total state space volumes of the exponential valleys are smaller than the ones of the power-law valleys, and thus the power-law valleys would be expected to draw a larger amount of probability than the exponential ones even when the trapping transition occurs. In order to investigate this issue more closely, we have studied three different combinations (cases F, G and H) of a power-law valley (valley 2) with an exponential valley (valley 1), where both valleys contain

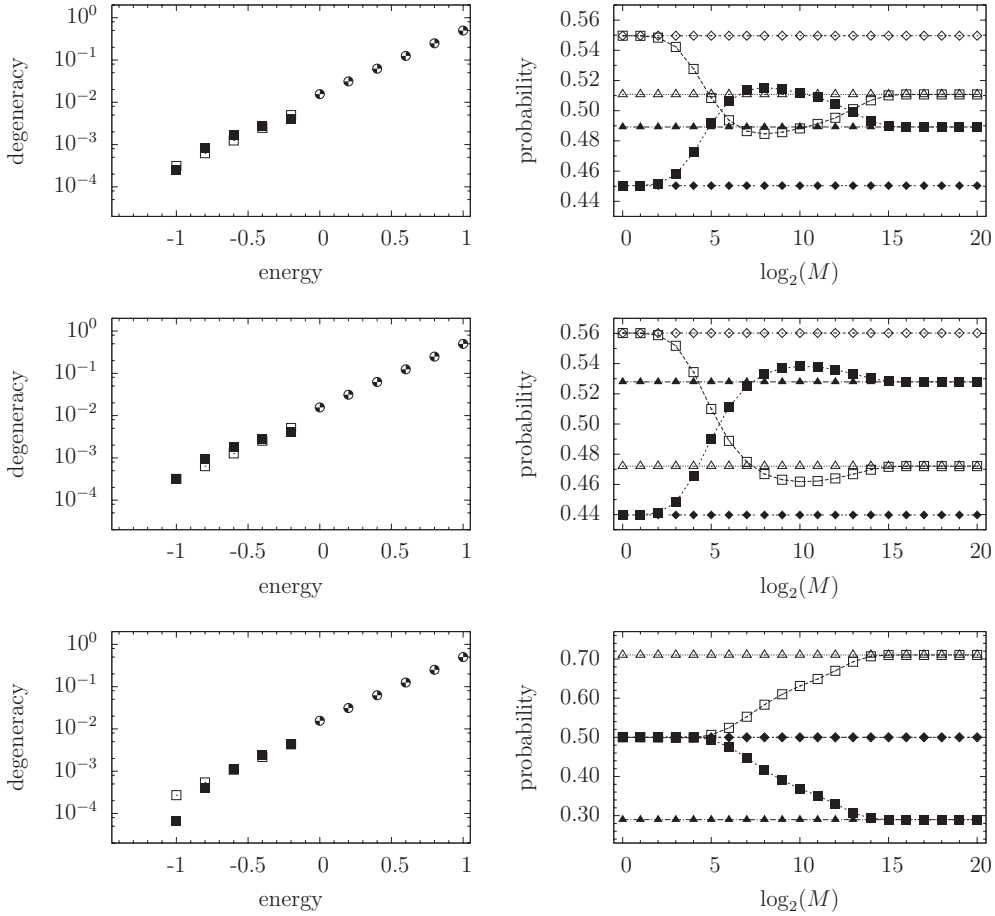

Figure 7. The degeneracy versus energy (left), and the quenched probabilities as a function of M (right) for the cases F (top), G (middle) and H (bottom). Notation as in figure 2.

the same total number of states, and where the super-valley above the saddle point exhibits an exponentially increasing density of states.

In case F (figure 7 (top left)), equality of the valley volumes is achieved by keeping the same power-law exponent as in figure 5 (top right), and scaling the degeneracies of all the nodes in the power-law valley by the same factor. Additionally, the exponent γ is chosen the same as in figure 5 (top right); the two valleys have more or less the same degeneracy at their lowest as well as at their topmost nodes.

Next, in cases G (figure 7 (middle left)) and H (figure 7 (bottom left)), the power-law exponents of valley 2 have been adjusted such that the state space volumes are the same and the degeneracies at the bottom and the top, respectively, are the same in the power-law and the exponential valley.

We find that in all three cases the bulge in the power-law density of states partway down the valley is still present, like in case D, i.e. the degeneracy of some of the power-law valley's nodes is higher than the one of the corresponding nodes of the exponential valley. This influences the dynamics at intermediate annealing speeds as shown in figure 7 (right), where the power-law valley draws more of the probability than contained in the equilibrium

probability distribution at the final temperature ($T = 0.1$). In figure 7 (bottom right) the effect is only very small but still noticeable.

4. Discussion and summary

In this study, we have analyzed the influence of a complex state space's energetic, entropic and kinetic features on the relaxation dynamics at finite time scales. We find that while extremely slow (global equilibrium) relaxation will lead to the establishment of a global Boltzmann distribution, of course, relaxation of a system with a complex barrier structure on realistic (i.e. small compared to the global equilibration time) time scales will lead to the trapping of probability in certain regions of state space. This is due to the lack of equilibrium both on a global level and even within the sub-valleys of the full landscape, combined with the strong interplay between entropic, energetic and kinetic features of the competing sub-valleys that control the flow of probability on the landscape.

In particular, we compare the trapping power of a valley with a power-law density of states to the one for a valley with an exponentially growing density of states. The outcome of this competition crucially depends on the annealing speed and shows that the clear distinction between these two paradigmatic densities of states observed at very slow (near-equilibrium) annealing is lost for fast non-equilibrium processes, and that the outcome of the relaxation can strongly depend on the time scale of the process and subtle features of the densities of states. In particular, the downward flow of probability within one single valley appears rather similar at fast annealing speeds for exponential and power-law valleys of comparable total size, as long as the trapping temperature of the valley with the exponential DoS is included in the temperature interval of the annealing process. This lack of a clear quantitative (not necessarily qualitative) difference between the probability flows in power-law and exponential DoS valleys is quite surprising and demonstrates that the usual reliance on equilibrium-type arguments when analyzing the dynamics on complex landscapes can be misleading when applied to finite time scale processes.

Traditionally, one has contrasted the outcome of an instantaneous quench with the result of an infinitely long annealing process. While in the first case the resulting probability distribution only depends on the rim sizes of valleys at the connecting saddle regions, where the probability flow splits, in the latter case, the final probability distribution should be concentrated only on the deepest minimum or minima. When extending this kind of analysis to finite time processes, one has typically assumed that there should be a smooth deformation of the infinitely-fast-quench probability distribution to the global Boltzmann distribution, leading to a monotonic decrease/increase of probability in the competing valleys with increasing annealing time. However, in earlier work [17], it was already shown that for a competition among valleys with exponentially growing densities of states but with different trapping temperatures and different kinetic factors, inversion effects could appear, i.e. the total amount of probability that reaches a given valley does not monotonically change with annealing time, e.g. a low-energy state that can be reached with reasonable probability at very slow annealing speeds can also be found with a similar or even higher probability by very fast annealing but not at an intermediate speed. In this work, we have shown that such inversions can also appear when exponential and power-law-like valleys are in competition, i.e. such effects can also be due to features in the local densities of states, and do not require a strong variation in the micro-connectivity of the landscape. We find that, depending on the details of the local densities of states, a local maximum or a local minimum of the final probability inside a valley can exist as a function of the annealing speed. However, we note that, even for the rather simple DoS we have

employed, there can already appear both a local maximum and a local minimum in the total amount of probability inside a given valley as a function of the annealing speed.

Such inversion effects are closely related to the phenomenon of preferential trapping, which denotes the fact that even in non-equilibrium situations (characterized by fast annealing) where the outcome should resemble the one of an instantaneous quench, the probability of reaching the deeper minima is greatly enhanced. Such preferential trapping was shown to be present for competing valleys with exponential DoS (and constant kinetic factors) [5]. In this work, we show that such preferential trapping is not only restricted to valleys with exponential densities of states, but also occurs for power-law-only systems or if different entropic features, i.e. different growth laws (and possibly mixtures thereof) within different sub-valleys, happen to co-exist within one system.

Considered from a more general perspective, where one tries to deduce simple heuristic rules to help us understand the dynamical features of energy landscapes in an intuitive fashion, the state space structure of complex systems and their relaxation behavior have in the past been captured by hypotheses like *deep valleys have large rims* [9] or *deep valleys relax fast* [17]. An additional heuristic like *exponential valleys attract last (but if they do they relax very fast)* might be helpful in order to explain the dynamics in many special landscapes in a simple qualitative fashion.

These new insights into fundamental aspects of the dynamics on complex landscapes could have far reaching consequences for scientific and technological applications that depend on understanding and controlling the state space dynamics of complex systems. Clearly, special measures have to be taken in order to prevent being trapped in the 'wrong' part of the state space and conversely to improve the funneling toward the 'right' valley. Further research within this area should address problems like determining unique classifications for the type of valleys that can be present (and possibly have been observed) in coarse-grained state spaces, going beyond the prototypical two-sub-valley systems by studying the effects of multi-basin interactions, or designing moveclasses for stochastic optimization methods such as the simulated annealing algorithms, which can take advantage of the differences in the trapping behavior of various types of valleys to achieve a faster convergence to the global and other deep-lying minima. As a final thought, one should recall that in many systems in materials science and chemistry, the global minimum modification is not necessarily the one with the most exciting physical properties, and thus developing search methods that can identify all stable low-energy minima of a system constitutes an important effort in theoretical chemistry and physics [36]. Here, in particular, being able to steer the global search or the experimental synthesis to many different stable minima by exploiting preferential trapping and inversion effects such as the ones demonstrated in this study will be of great value.

References

[1] Hoffmann K H and Sibani P 1988 Diffusion in hierarchies *Phys. Rev.* A **38** 4261–70
[2] Wales D J 2003 *Energy Landscapes (Cambridge Molecular Science)* (Cambridge: Cambridge University Press)
[3] Benkovic S J, Hammes G G and Hammes-Schiffer S 2008 Free-energy landscape of enzyme catalysis *Biochemistry* **47** 3317–21
[4] Frauenfelder H, McMahon B H, Austin R H, Chu K and Groves J T 2001 The role of structure, energy landscape, dynamics, and allostery in the enzymatic function of myoglobin *Proc. Natl Acad. Sci. USA* **98** 2370–4
[5] Schön J C 1997 Preferential trapping on energy landscapes in regions containing deep-lying minima—the reason for the success of simulated annealing? *J. Phys. A: Math. Gen.* **30** 2367–89
[6] Dobson C M, Šali A and Karplus M 1998 Protein folding: a perspective from theory and experiment *Angew. Chem. Int. Ed.* **37** 868–93

[7] Kirkpatrick S, Gelatt C D Jr and Vecchi M P 1983 Optimization by simulated annealing *Science* **220** 671–80
[8] Černý V 1985 Thermodynamical approach to the travelling salesman problem: an efficient simulation algorithm *J. Optim. Theory Appl.* **45** 41–51
[9] Salamon P, Frost R and Sibani P 2002 *Facts, Conjectures, and Improvements for Simulated Annealing* (*Monographs on Mathematical Modeling and Computation* vol 7) 1st edn (Philadelphia, PA: SIAM)
[10] Corey E J 1991 The logic of chemical synthesis: multistep synthesis of complex carbogenic molecules *Angew. Chem. Int. Edn* **30** 455–65
[11] Schön J C and Sibani P 1998 Properties of the energy landscape of network models for covalent glasses *J. Phys. A: Math. Gen.* **31** 8165–78
[12] Schön J C and Jansen M 1996 A first step towards planning of syntheses in solid state chemistry: determination of promising structure candidates using global optimization *Angew. Chem. Int. Edn* **35** 1286–304
[13] Wales D J, Doye J P K, Miller M A, Mortenson P N and Walsh T R 2000 Energy landscapes: from clusters to biomolecules *Adv. Chem. Phys.* **115** 1–115
[14] Geman S and Geman D 1984 Stochastic relaxation, Gibbs distribution, and the Bayesian restoration of images *IEEE Trans. Pattern Anal. Mach. Intell.* **6** 721–41
[15] Levinthal C 1968 Are there pathways for protein folding? *J. Chim. Phys. Phys.-Chim. Biol.* **65** 44–5
[16] Bryngelson J D, Onuchic J N, Socci N D and Wolynes P G 1995 Funnels, pathways, and the energy landscape of protein folding: a synthesis *Proteins: Struct. Funct. Genet.* **21** 167–95
[17] Hoffmann K H and Schön J C 2005 Kinetic features of preferential trapping on energy landscapes *Found. Phys. Lett.* **18** 171–82
[18] Klotz T and Kobe S 1994 Exact low-energy landscape and relaxation phenomena in Ising spin glasses *Acta Phys. Slovaca* **44** 347
[19] Becker O M and Karplus M 1997 The topology of multidimensional potential energy surfaces: theory and application to peptide structure and kinetics *J. Chem. Phys.* **106** 1495–517
[20] Ball K D and Berry R S 1998 Realistic master equation modeling of relaxation on complete potential energy surfaces: partition function models and equilibrium results *J. Chem. Phys.* **109** 8541–56
[21] Ball K D and Berry R S 1998 Realistic master equation modeling of relaxation on complete potential energy surfaces: kinetic results *J. Chem. Phys.* **109** 8557–72
[22] Schön J C, Wevers M A C and Jansen M 2003 'Entropically' stabilized region on the energy landscape of an ionic solid *J. Phys.: Condens. Matter* **15** 5479–86
[23] Kobe S and Krawczyk J 2004 Relationship between energy landscape and low-energy dynamics of $\pm J$ spin glasses *J. Magn. Magn. Mater.* **272–276** 1284–5
[24] Derrida B 1981 Random-energy model: an exactly solvable model of disordered systems *Phys. Rev.* B **24** 2613–26
[25] Sibani P and Schriver P 1994 Local phase-space structure and low-temperature dynamics of short range Ising spin glasses *Phys. Rev.* B **49** 6667–71
[26] Sibani P, Schön J C, Salamon P and Andersson J-O 1993 Emergent hierarchical structures in complex system dynamics: a phase space analysis of the travelling salesman problem *Europhys. Lett.* **22** 479–85
[27] Schön J C 2002 Energy landscape of two-dimensional lattice polymers *J. Phys. Chem.* A **106** 10886–92
[28] Klotz T, Schubert S and Hoffmann K H 1998 The state space of short-range Ising spin glasses: the density of states *Eur. Phys. J.* B **2** 313–7
[29] Schubert S and Hoffmann K H 2006 The structure of enumerated spin glass state spaces *Comp. Phys. Commun.* **174** 191–7
[30] Hoffmann K H, Fischer A, Schubert S and Streibert T 2006 Modelling aging experiments in spin glasses *Parallel Algorithms and Cluster Computing* (*Lecture Notes in Computational Science and Engineering* vol 52) ed K H Hoffmann and A Meyer (Berlin: Springer) pp 281–302
[31] Fischer A 2008 Modelling complex systems: tree structures *Dissertation* Technische Universität Chemnitz, Germany
[32] Stillinger F H and Weber T A 1982 Hidden structure in liquids *Phys. Rev.* A **25** 987–9
[33] Hoffmann K H, Schubert S and Sibani P 1997 Age reinitialization in hierarchical relaxation models for spin-glass dynamics *Europhys. Lett.* **38** 613–8
[34] Klotz T, Schubert S and Hoffmann K H 1998 Coarse graining of a spin-glass state space *J. Phys.: Condens. Matter* **10** 6127–34
[35] Metropolis N C, Rosenbluth A W, Rosenbluth M N, Teller A H and Teller E 1953 Equation of state calculations by fast computing machines *J. Chem. Phys.* **21** 1087–91
[36] Schön J C, Doll K and Jansen M 2010 Predicting solid compounds via global exploration of the energy landscape of solids on the *ab initio* level without recourse to experimental information *Phys. Status Solidi* B **247** 23–39